

High-pressure studies of Jahn-Teller-split luminescence in alkali halides doped with In^+ and Tl^+

David Klick and H. G. Drickamer

Department of Physics, School of Chemical Sciences, and Materials Research Laboratory, University of Illinois at Urbana-Champaign, Urbana, Illinois 61801*

(Received 20 September 1977)

Measurements of steady-state intensity and lifetime were made over a range of pressures (4–60 kbar) and temperatures (100–300°K) for five alkali-halide crystals doped with In^+ and Tl^+ . The emission spectrum is a doublet (or a triplet in the case of CsI:Tl), caused by a Jahn-Teller splitting of the excited state. The relative intensity distribution of the spectral peaks as a function of temperature and pressure determines the parameters for a model of two levels in "dynamic equilibrium." The same model predicts lifetime changes with temperature and pressure which are in excellent agreement with the data for the In^+ -doped compounds. For the Tl^+ -doped compounds, metastable states control the lifetime, and parameters are extracted from the data for a multilevel model. Level splittings, level degeneracies, and intrinsic radiative rates are among the parameters determined in this study.

I. INTRODUCTION

Jahn-Teller (JT) splitting of the relaxed excited states of heavy-metal ions in alkali halides has been widely studied and analyzed. The contributions of Fukuda¹⁻³ and Ranfagni⁴⁻⁷ have been especially significant. Aspects of their work are important for high-pressure studies have been summarized by Drotning⁸; his discussion will not be repeated here, except to point out that, for excitation in the A band, a doublet emission is observed.

The $^3T_{1u}$ state generally splits into two levels, X and T, with a higher-energy emission originating from the T level. (However, a situation has been found⁸ in CsI:Tl at 25 kbar, where emission occurs from three levels.) The metastable state $^3A_{1u}$ is expected to split in a similar manner, leading to a trap level under each emitting level. Steady-state emission is not affected by the traps, but decay curves may be. There have been a number of decay studies at atmospheric pressure.^{1,9-11} Assignment of symmetry and degeneracy to the levels appears to be a matter of some dispute.¹⁻⁷

Drotning⁸ made extensive measurements of the relative emission intensities from the T and X levels as functions of pressure at room temperature. We have extended his studies in two ways: we measure both intensities and lifetimes, and we make measurements at various pressures over a temperature range of 100–300°K. The experimental techniques and methods of sample preparation are discussed elsewhere.¹²⁻¹⁵ Host lattices were doped with 0.01 mole% of In^+ or Tl^+ impurity. Spectral peaks were fit with symmetric Gaussians except for peak 3 in CsI:Tl , which is skewed because of quadratic coupling.¹² A typical set of low-

temperature corrected spectra is shown in Fig. 1 (KCl:In at 31 kbar). All decay curves were single exponential, except when traps appeared. In that case, there is a nonequilibrium fast component of exceedingly short lifetime; the fast component was blocked during data taking by a time gate, and the slow component was fit with a single-exponential function.

Low-temperature (LT) spectral studies tell us about the size of the JT level splitting versus pressure. The ratio of peak areas is regulated by a Boltzmann factor that depends on the splitting. In conjunction with LT studies, lifetimes versus pres-

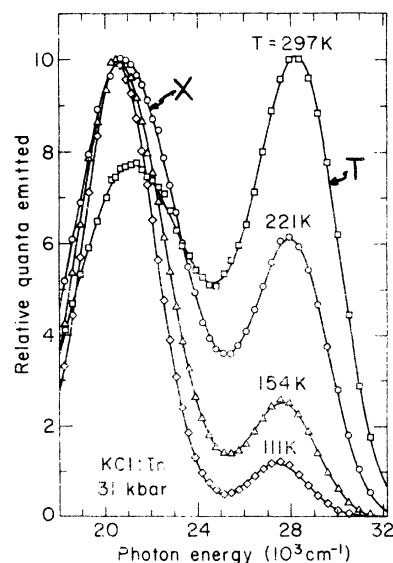


FIG. 1. Spectra of KCl:In at 31 kbar for several temperatures.

sure can determine the level degeneracies and the radiative rates of the two states. Measurements of lifetime versus temperature provide checks on the parameters already derived or, when there are nonemitting levels, determine trap depths. Hydrostatic pressure studies (to 10 kbar) of KBr:In and KI:In have been performed: Fukuda² measured LT spectra and Niilisk¹⁶ measured lifetimes in general agreement with our results

II. ANALYSIS

Drotning found that the most striking effect of pressure is a redistribution of intensity within the JT-split-emission doublet. As pressure increases, the high-energy T peak invariably gains intensity at the expense of the low-energy X peak. Identical behavior is seen in the face-centered-cubic (fcc) and simple cubic (sc) phases of alkali halides, so that no distinction will be made between phases here. (Drotning used primes to denote the sc phase.)

Some of Drotning's data are reproduced in Fig. 2. Here the fraction of total doublet emission in the low-energy X peak (to be referred to as % X) is plotted as a function of pressure. The intensity of peak X drops as peak T grows in, for all the indium-doped potassium halides (except fcc KCl:In), in both phases. (Potassium halides undergo a phase transition from the fcc to the sc structure at a pressure of about 20 kbar.) The curves in Fig. 2 are calculated from a model to be presented in this paper; the curves, derived from independent data, are in good agreement with Drotning's data points.

With the introduction of low-temperature and transient high-pressure measurements, a new theory is proposed that best describes all sets of data, including Drotning's.⁸ It will be called the "dynamic equilibrium" model (in quotes because an excited system cannot be in true equilibrium). It is

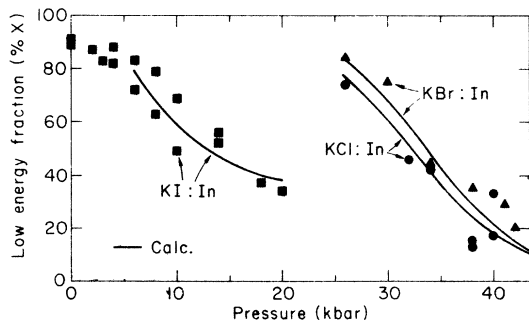


FIG. 2. Fraction of emission in low-energy peak of indium-doped potassium halides at room temperature vs pressure. Drotning's points and curves calculated from independent data presented here.

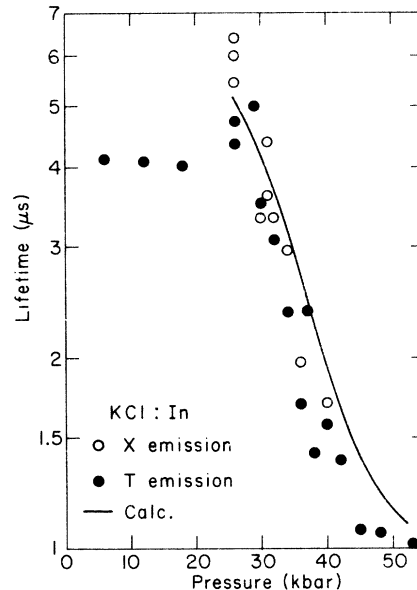


FIG. 3. Lifetime change with pressure for KCl:In at room temperature.

assumed that rearrangement of excitation among the levels is much faster than deexcitation.

For the In⁺-doped potassium halides (KH:In), a two-level model is sufficient to describe the data. Consideration of nonradiative deexcitation, non-emitting levels (traps), and three-peak phosphors will be deferred until Sec. IV. In general, the two levels may have different intrinsic radiative lifetimes and degeneracies. However, for two levels in "dynamic equilibrium," both emission peaks must have identical, single-exponential decay curves. This is confirmed in Fig. 3, which is a plot of room-temperature (RT) lifetime versus pressure for KCl:In. The open circles (measured at peak X) and the filled circles (measured at peak T) lie on the same curve in the sc phase. Note that in the fcc phase, where only one peak (T) is seen, the lifetime (which is intrinsic to the T level) is unchanged by pressure. Fortunately, this holds generally true in KH:In; pressure strongly affects the size of the JT splitting and very little else.

If n is the occupation of a level, the population ratio (n_T/n_X) of the two levels in "dynamic equilibrium" is simply given by a Boltzmann factor involving the level degeneracy g and the JT splitting $\Delta E = E_T - E_X$. The Boltzmann factor is denoted K , and is given in Eq. (1). [Equations (1)–(3) are collected in Table I.] K is not a constant, but a function of temperature and pressure (through ΔE). By simple kinetic arguments, it is found that the decay curve in a single exponential function, with a lifetime τ given by Eq. (2). Here k_X and k_T are radiative rate constants intrinsic to each level, and

TABLE I. Equations for a two-level Jahn-Teller system.

<p>“Dynamic equilibrium”: $k_A, k_B \gg k_X, k_T$.</p> <p>(1) $(k_A/k_B) = (n_T/n_X) = (g_T/g_X) \exp(-\Delta E/kT) = K$.</p> <p>(2) $\frac{1}{\tau} = (k_X + Kk_T)/(1 + K)$, $\%X = 1/(1 + Kk_T/k_X)$.</p> <p>(3) $\log_{10}[(1/\%X) - 1] = -\Delta E \log_{10} e (kT)^{-1} + \log_{10} \left(\frac{g_T k_T}{g_X k_X} \right)$.</p>

$k_X^{-1} = \tau_X$. The intrinsic rates k_X and k_T were found to be constant, so the temperature and pressure dependence of the lifetime is contained only in K .

In a similar manner, one can solve for the ratio of steady-state peak areas. This ratio is given in Eq. (2), expressed as the low-energy fraction $\%X$. Again, the temperature and pressure dependence of $\%X$ is contained in K . Decay and steady-state measurements are linked by Eq. (2), and therefore one measurement can predict the other.

In room-temperature studies, Drotning proved that an X -dominated spectrum invariably becomes T dominated at higher pressures (unless, say, a phase transition intervenes). He postulated that the T level was stabilizing with respect to the X level. We retain this postulate, as shown in Fig. 4, and extend it to argue that the T level actually drops to a lower energy than the X level at high pressure. The evidence, which will be shown later, is that at high pressure $\%X$ drops as the temperature is lowered.

It is expected from theory^{3,7} that the relaxed excited state will have potential minima at different values of the totally symmetric coordinate Q , as depicted in Fig. 4. Both minima are at larger volume Q than the ground state, leading to the shifts with pressure of emission peak maxima to higher energy seen by Drotning.¹² Excitation from the ground-well bottom is to the T level (as is known from ultralow-temperature studies),¹ and emission is from both excited wells, with peak-energy maxima $h\nu_T$ and $h\nu_X$. Due to the Stokes's shift as illustrated in Fig. 4 $h\nu_T - h\nu_X$ is on the order of 5000 cm^{-1} . The T - X level splitting is minute in comparison (less than 500 cm^{-1}), so that even when the T level is lower than the X level, the T emission is at higher energy.

Note that ΔE is defined as $E_T - E_X$, which is negative at high pressure. By Eq. (1) then, K can vary

from about zero to very large as the pressure is increased. At some pressure p_0 , $\Delta E = 0$ and the levels are no longer split. By Eq. (1), K is g_T/g_X and the temperature dependence disappears from the equations for τ and $\%X$, at this pressure. A good check of the theory and assumptions on which it rests, is to measure $\tau(p_0)$ and $\%X(p_0)$ as functions of temperature to prove that they are constant. This was done with good results, as will be shown.

Let us examine the limiting behavior of Eq. (2). As pressure increases at room temperature, K can vary from zero (at low pressure) to infinity (at high pressure). Then at low pressure, $\tau = \tau_X$ and $\%X = 1$, while at high pressure, $\tau = \tau_T$ and $\%X = 0$. Drotning already found that $\%X$ drops from one to zero. It will be shown that the lifetime does vary (in fact drop) from τ_X to τ_T as pressure rises.

The behavior of K with temperature depends on ΔE . At pressures below p_0 , ΔE is positive, so K rises with increasing temperature; then by Eq. (2), $\%X$ drops as the temperature rises (as in Fig. 1). At p_0 , K is constant with temperature, and so are τ and $\%X$. Above p_0 , ΔE is negative and K drops with increasing temperature; then $\%X$ actually rises with the temperature. This kind of limiting behavior with temperature and pressure predicted by the theory is seen in all the KH:In.

The assumption behind the theory are as follows: (i) there is “dynamic equilibrium,” which is supported by decay measurements; (ii) the barrier height between the T and X states is negligible in our temperature range. Fukuda¹ claims that the barrier generally becomes important only below about 80°K. In KRR:In and CsI:Tl, strange LT (below 130°K) behavior in our data could be due to barrier effects; (iii) the excited system consists of just two emitting states; (iv) The splitting ΔE is

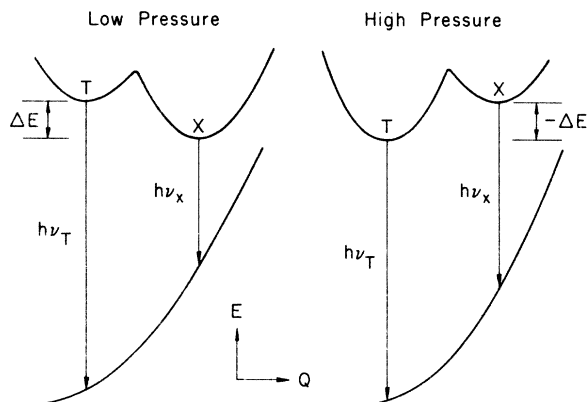


FIG. 4. Schematic diagram of Jahn-Teller-split excited state at low and high pressures.

constant with temperature; and (v) intrinsic radiative rates k_X and k_T , and level degeneracies g_X and g_T are constant with temperature and pressure. These assumptions turned out to hold true for the three indium-doped potassium halides tested. Indirect proof lies in the fact that the model is in excellent agreement with the data. Experiments to test the assumptions directly were also performed.

Before the data are displayed, the method of presentation that best fits the theory must be decided. The major steady-state measurement is that of low-energy fraction $\%X$ vs temperature. Its theoretical variation, given in Eq. (2), can be rearranged as in Eq. (3), where log means common log. If the quantity on the left is plotted against $(kT)^{-1}$, a straight line of slope $(-\Delta E \log_{10} e)$ and intercept $\log_{10}(g_T k_T / g_X k_X)$ should result. Such a graph (which, like an Arrhenius plot, decomposes the Boltzmann factor) will be called a "steady-state plot." If assumptions one to five are true within a particular crystal phase, lines at different pressures will meet at a common intercept, and their slopes will increase systematically with pressure as ΔE drops. When $\Delta E = 0$ at p_0 , the line is horizontal.

The procedure is to take LT data at several pressures and draw a steady-state plot. Lines having a common intercept are drawn (by eye) through the data. The slopes show what ΔE is as a function of pressure and, by interpolation, which pressure is p_0 . The intercept gives the ratio of degeneracies times the ratio of intrinsic radiative rates of T to X . The literature is divided on the subject of degeneracy assignments, so the g values that best fit the lifetime data are used.

If the degeneracies are known, the intercept of the steady-state plot gives the ratio of intrinsic radiative lifetimes. Then one need only determine either τ_X or τ_T to know the other. At RT, one can go to very low pressure, where $\tau = \tau_X$, or very high pressure, where $\tau = \tau_T$. If the extreme-pressure (where emission is pure) X or T cannot be reached at RT, it can often be reached at LT. With k_X and k_T determined, and the $\Delta E(p)$ known from a steady-state plot, one can use Eq. (2) to generate curves $\tau(p)$ and $\tau(T)$ corresponding to the three most likely degeneracy assignments ($g_X/g_T = 2, 1, \text{ or } 0.5$). One of these three sets of curves will typically fit the data much better than the other two, so that the degeneracy assignment is obvious. Finally, a curve $\%X(p)$ is generated from Eq. (2), and fit to Drotning's completely independent data as in Fig. 2. If the model predicts all four sets of data $\%X(T)$, $\%X(p)$, $\tau(T)$, and $\tau(p)$ within reasonable accuracy, one can be confident that one has the right set of parameters g_T , g_X , k_T , k_X , and $\Delta E(p)$.

III. INDIUM-DOPED POTASSIUM HALIDES

The two-level "dynamic equilibrium" model was applied (following the procedure just described) to sc KCl:In, sc KBr:In, and fcc KI:In, with very good results. KCl:In is probably the best example, so application of the model to KCl:In will be fully explained, and any differences for KBr:In and KI:In will be mentioned.

Figure 5 shows a steady-state plot of sc KCl:In. The abscissa is $(kT)^{-1}$ in units eV^{-1} . Temperature ($^\circ\text{K}$) is given at the top of the plot. The ordinate is $\log_{10}[(1/\%X) - 1]$; for reference, the values of $\%X$ corresponding to ordinate marks will be given: (1.2, 6%), (0.8, 14%), (0.4, 28%), (0, 50%), (-0.4, 72%), (-0.8, 86%), and (-1.2, 94%). Measurement of $\%X < 15\%$ or $85\% < \%X$ is difficult because of small peaks. Therefore, the steady-state plot can only contain data from pressures close to p_0 , for which $\%X$ does not reach extreme values at low temperatures. Because of the strong dependence of ΔE on pressure (reflected in the swiftly increasing slopes of Fig. 5), great care was taken in setting the pressure.

From Fig. 5 are found the level splittings ΔE at three pressures (see Table II). Splittings are on the order of tens of millielectron volts or hundreds of wavenumbers. The three values of ΔE are fit with a line, giving an equation for the function $\Delta E(p)$. The pressure p_0 at which $\Delta E = 0$ is found to be about 38 kbar, where $\%X = 24\%$ (as calculated from the intercept). From the intercept (0.5), $g_T \tau_X / g_X \tau_T$ is found to be 3.16. Since at high pres-

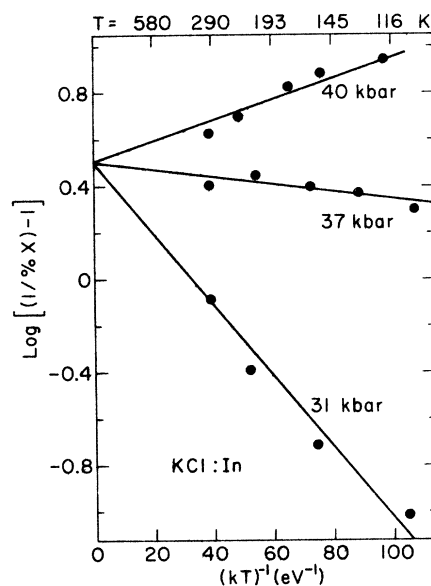


FIG. 5. Steady-state plot of KCl:In above the phase transition.

TABLE II. Jahn-Teller-level splitting (ΔE) as a function of pressure.

Compound	Pressure (kbar)	ΔE (meV)
KCl:In	31	35
	37	3.7
	40	-10.1
KBr:In	34	43
	37	21.0
	40	6.9
	43	-5.6
KI:In	6	66
	10	42
	15	27.5
	20	20.0
KBr:Tl	4	24.9
	10	-4.4
CsI:Tl	32	38.5
	37	16.1

sure $\tau(p)$ levels off to about $1 \mu\text{sec}$ (see Fig. 3), and at lower pressures the lifetime rises higher than 3.16, it is clear that $g_X/g_T=2$. Then $\tau_T=1 \mu\text{sec}$ and $\tau_X=6.32 \mu\text{sec}$ (see Table III). If sc KCl:In extended below the phase transition at about 20 kbar, $\tau(p)$ would presumably level off at $6.32 \mu\text{sec}$, giving a sigmoid-type curve.

These values for k_X , k_T , g_X , g_T , and $\Delta E(p)$ were inserted in Eq. (2) and the curve in Fig. 3 was generated. This curve is not a fit to the data, but a calculation based mainly on parameters from the steady-state plot. Discrepancies can be attributed to some uncertainties in k_X and k_T and especially the linear approximation to $\Delta E(p)$. Since ΔE was measured only at 31, 37, and 40 kbar, the agreement between theory and experiment as low as 26 kbar and as high as 52 kbar is surprisingly good. At several pressures for KCl:In, $\tau(T)$ was measured. Its trend was in agreement with calculations from Eq. (2). Specifically, at $p_0=38$ kbar and at $p=53$ kbar, where the lifetime is expected to be constant with temperature, it was constant

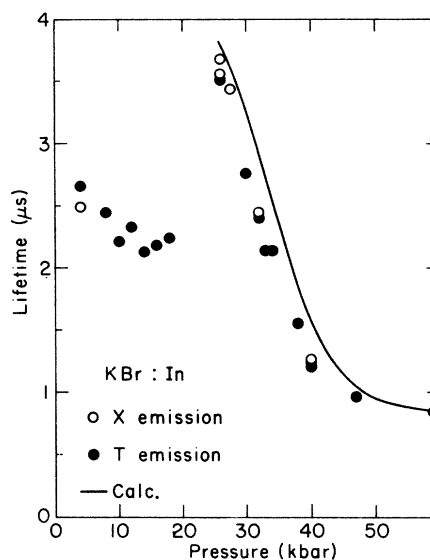


FIG. 6. Lifetime change with pressure for KBr:In at room temperature.

within 20%, confirming assumptions of the theory.

Similar sets of data were taken for KBr:In and KI:In. In these two compounds, the X and T peaks are found in both phases, but in only one phase is a complete treatment of the problem possible. In fcc KBr:In, p_0 is at about 4 kbar, so that emission has almost completely converted to the T peak in our pressure range. Steady-state and lifetime measurements were taken to low temperatures at 4 kbar: $\%X(p_0)$ was found to be constant at 30%, and $\tau(p_0)$ was constant (within 10%) at $2.37 \mu\text{sec}$. This again supports the model, which predicts an absence of temperature effects at p_0 . Emission is completely converted to peak T by 18 kbar; τ_T was measured to be $2.0 \mu\text{sec}$ at 18 kbar and to be constant within 5% to low temperatures as expected. The RT lifetime drops with pressure slightly in fcc KBr:In, indicating that the emission is converting to peak T and that $\tau_X > \tau_T$. It can sketchily be determined that $\tau_X/\tau_T=2.6 \pm 0.3$ and $g_X/g_T=1$.

In sc KBr:In, the intercept parameters g_X/g_T ,

TABLE III. Measured Jahn-Teller parameters.

Crystal	Structure	$\log_{10}(g_T\tau_X/g_X\tau_T)$	τ_X (μsec)	τ_T (μsec)	g_X/g_T	p_0 (kbar)	$\%X(p_0)^a$	$\tau(p_0)^a$
KCl:In	sc	0.5	6.32^b	1.0	2	38	24	2.28
KBr:In	sc	0.72^b	4.37	0.837	1	42	16	1.40
KI:In	fcc	0.55	2.9	0.82^b	1^c	>20	22	1.28
KBr:Tl	fcc	0.7	0.10	0.010	2^c	9	17	
CsI:Tl	sc	0.87	$\tau_2/\tau_3=7.4$		1^c	41	$\%2=12$	

^a Calculated from Eq. (2).

^b This one of the three [τ_X , τ_T , or $\log_{10}(g_T\tau_X/g_X\tau_T)$] was calculated from the two that were measured.

^c Degeneracy assignment is not certain.

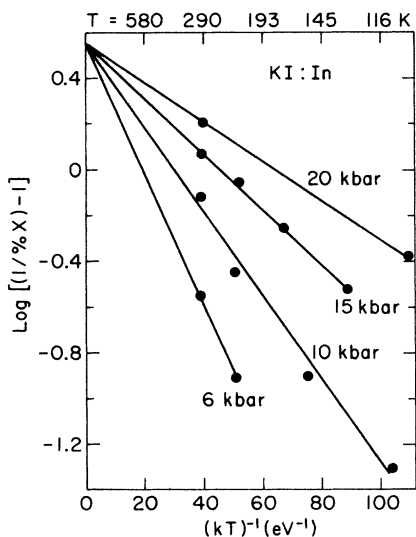


FIG. 7. Steady-state plot for KI:In below the phase transition.

τ_T , and τ_X are all determinable from lifetime measurements (see Fig. 6). At a very high pressure (59 kbar), τ_T was found to be $0.837 \mu\text{sec}$. Low-temperature lifetimes at 26 kbar (where $\%X \sim 100\%$) yielded a constant value of $\tau_X = 4.37 \pm 0.1 \mu\text{sec}$. Thus $\tau_X/\tau_T = 5.22$ and $\log_{10}(\tau_X/\tau_T) = 0.72$. The intercept of the steady-state plot, given by $\log_{10}(g_T\tau_X/g_X\tau_T)$, must be near 0.72, so it is clear that $g_X/g_T = 1$. In this case, then, direct measurements of τ_X and τ_T determine the steady-state intercept. Lines are fit to the steady-state data, giving four values for $\Delta E(p)$. These are again joined by a best-fit line for purposes of extrapolation, and a curve of

$\tau(p)$ is generated from $\Delta E(p)$. As seen in Fig. 6, calculation deviates from experiment by a small, constant amount; it appears that if our value of p_0 were one kbar lower, the curve would lie right on the data!

For sc KI:In, p_0 is too far above 44 kbar to make a steady-state plot. A complete study, however was performed on fcc KI:In, despite the fact that $p_0 > 20$ kbar (above the phase transition). The steady-state plot is shown in Fig. 7. An intercept of 0.55 means that $g_T\tau_X/g_X\tau_T = 3.55$. Degeneracies of $g_X/g_T = 1$ best fit the lifetime data $\tau(p)$ and $\tau(T)$, but the improvement over other degeneracy assignments was not as obvious as in KCl:In and KBr:In. The slopes of Fig. 7 give $\Delta E(p)$ at four pressures; unlike KCl:In and KBr:In, $\Delta E(p)$ was clearly non-linear (see Table II). Therefore, all calculations involving ΔE were done at four pressures and the results were then joined by a smooth curve.

The curve in Fig. 8 is such a smooth curve. Agreement with experiment is good. To calculate $\tau(p)$, either τ_X or τ_T had to be found. At 6 kbar $\%X \approx 1$ for low temperatures, so that $\tau \approx \tau_X$. Figure 9 shows $\tau(T)$ at 6 kbar; the lifetime appears to approach an LT limit of about $\tau_X = 2.9 \mu\text{sec}$, in agreement with Fukada's atmospheric pressure value of $\tau_X = 3 \mu\text{sec}$.¹ This value was used with the steady-state intercept to calculate $\tau_T = 0.82$. With all parameters known, theoretical curves were generated for Figs. 8 and 9. Agreement with the data in Fig. 9 (especially the independent set at 15 kbar) is quite good.

To summarize the In⁺-doped potassium halides, they all are subject to the JT effect in both phases, except for fcc KCl:In. The pressure p_0 at which the JT splitting is zero rises in both phases in the se-

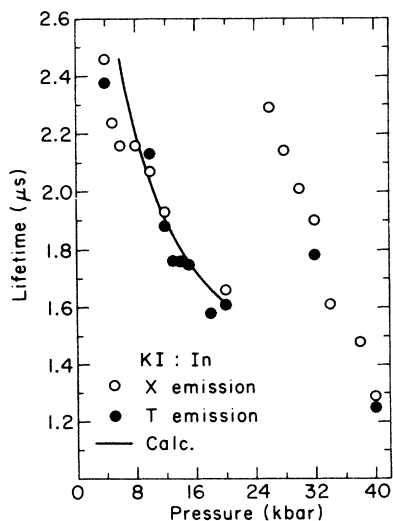


FIG. 8. Lifetime change with pressure for KI:In at room temperature.

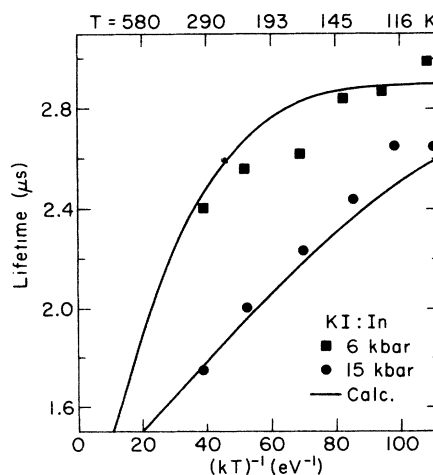


FIG. 9. Lifetime change with temperature for KI:In at 6 and 15 kbar.

TABLE IV. Lifetime at pressure p_0 in the two phases of KH:In.

Phase	$\tau(p_0)$ (μsec)		
fcc	(>4)	~ 2.37	1.28
sc	2.28	1.40	< 1.2
Crystal	KCl:In	KBr:In	KI:In

quence $p_0(\text{Cl}) < p_0(\text{Br}) < p_0(\text{I})$. The intrinsic lifetime of peak X (τ_X) is always greater than that of peak T (τ_T) by a factor of 3 to 6. Lifetimes are longer in the fcc phase than in the sc phase, as can be seen in Table IV.

Otherwise, the two phases give similar results. In all cases, X emission gives way to T emission with pressure according to the model proposed. This is due to a stabilization of the T minimum with pressure to the point where the T level is lower than the X level at high pressures. At the same time, the measured lifetime changes rapidly from τ_X to τ_T with pressure. The major difference among the crystals is the degeneracy assignment, where, without doubt, $g_X/g_T = 2$ for sc KCl:In, but $g_X/g_T = 1$ for sc KBr:In. It is generally thought¹ that the X level is doubly degenerate and the T level is nondegenerate. This would explain KCl:In. However, recent work that split the degeneracies with a magnetic field³ insists that the X and T levels are both doubly degenerate. This would explain the KBr:In result. Both schemes are theoretically allowed.⁶

At this point, the direct evidence supporting the assumptions within the model will be summarized. The assumption of "dynamic equilibrium" holds at RT for the three KH:In; this can be seen from the equivalence of lifetimes measured at peaks X and T in $\tau(p)$ plots. Also as the temperature is lowered, whichever level is more stable (X below p_0 , T above p_0) emits more and more of the light. (If the barrier were important, peak T would always rise as the temperatures fell. Barrier effects are occasionally seen at very low temperatures.)

The two-level model works well for KH:In. The level splitting is found to be constant with temperature, giving straight lines on the steady-state plots. Intrinsic radiative rates were found to be constant with temperature [as $\tau_T(T)$ as constant in sc KCl:In and fcc KBr:In, and $\tau_X(T)$ in sc KBr:In], and pressure [as $\tau(p)$ was constant in fcc KCl:In, NaCl:In, and sc KBr:Tl, where there is no JT effect]. The constancy of τ_X and τ_T with temperature was also proven in fcc KBr:In and sc KCl:In by monitoring $\%X$ and τ at p_0 to low temperatures. Thus, the assumptions behind the model can be considered proven in KH:In, and one could expect

them to hold true in other JT-split systems, such as the Tl⁺-doped crystals to be discussed in Sec. IV.

IV. THALLIUM-DOPED ALKALI HALIDES

It is known from the literature^{1,9-11} that the Tl⁺ lifetime is dominated even at RT by the metastable $^3A_{1u}$ levels (also by the JT split) that underlie the emitting levels. These traps had no effect on In⁺ lifetimes for two reasons (a) Trap depths appear to be quite small [e.g., 2.2 meV in KI:In.¹ (b) Intrinsic In⁺ lifetimes are slow (on the order of 1 μsec), so the temperature must be very low (e.g., 40°K for KI:In) before detrapping and not emission is the rate-limiting step. In contrast, Tl⁺ trap depths are tens of millivolts and intrinsic lifetimes are on the order of 10 nsec.

Before dealing with a JT-split emitting level with an underlying trap or traps, let us consider a single emitting level with a trap. If the two levels are in "dynamic equilibrium," one has a special case of the model just described. The lifetime is given by Eq. (2) with one of the k 's equal to zero.

However, in our case the wells cannot be in "equilibrium," since the decay is not single exponential. A fast and slow component are usually seen, even at temperatures as high as room temperature. After excitation to the emitting level (absorption to and emission from the metastable level are forbidden), some emission occurs immediately (faster than the very fast Tl⁺ intrinsic radiative rate). This fast component is quenched (speeded up and reduced in intensity) by the ability of most of the excitation to surmount an energy barrier and reach the trap. Detrapping occurs slowly, at a rate dependent on the ability of the excitation to surmount a higher barrier back to the emitting level and not be trapped again before emission. The resulting decay curve is a sum of two exponentials called the fast and slow components.

One can write the rate equations for this system. They yield a differential equation like the damped harmonic oscillator for the population of the emitting level. Instead of a damped oscillation, the solution is the sum of two decaying terms. To make the problem tractable, approximations are made for various temperature regions. At very low temperatures, it is as if the trap were not there. At very high temperature, the fast component is completely quenched, and the slow lifetime is twice the intrinsic lifetime of the emitting level.

What temperature regime are we in? One might guess that 100–300°K is a rather high temperature for most processes in inorganic crystals. The fast component typically has a much larger coefficient than the slow component, but it is so fast that the

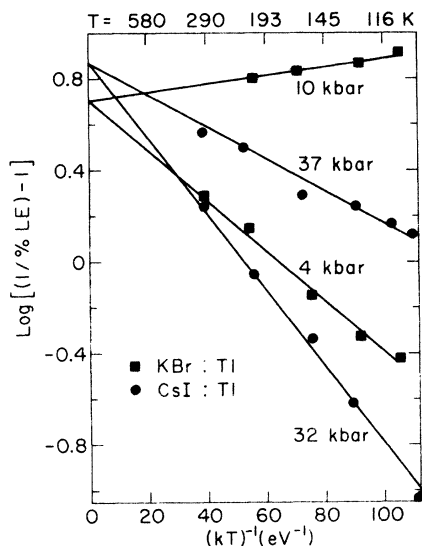


FIG. 10. Steady-state plots of KBr:Tl below the phase transition and CsI:Tl at high pressure. %LE refers to percent of low-energy peak present.

slow component dominates in total area. Since most of the emission is in the slow component, we are in the high-temperature regime.

Support for this statement comes from measurements of the amount of fast component versus temperature.¹⁷ In five doped alkali-halide crystals over our temperature range, the fast-component intensity is governed simply by a Boltzmann factor, where the energy in the exponent (on the order of 10–20 meV) is interpreted to be the barrier to trapping. Such a result can be derived from the equations only at high temperatures, where the rate of trapping is much faster than the intrinsic radiative rate.

Once the excitation is trapped, the system does attain "dynamic equilibrium." The Boltzmann factor for detrapping depends on the trap depth ϵ (energy difference between well bottoms), not the trap depth plus a barrier height. When the approximations appropriate for the high-temperature regime are made, the slow lifetime is found to be

$$\tau = \tau_{\text{rad}}(1 + e^{\epsilon/kT}) - \tau_{\text{rad}}e^{\epsilon/kT}, \quad (4)$$

where τ_{rad} is the intrinsic lifetime and $\epsilon \gg kT$. Equation (4) is just a special case of (2). In agreement with Trinkler and Plyavin,¹⁸ it is found that an "equilibrium" situation is attained soon after the fast component has disappeared. Their expression for a three-level system (X , T , and trap) is correct. However, theoretically^{3,6} one expects X and T to each have an underlying trap X_0 and T_0 . Let us develop a four-level model similar to the two-level model already described. Let ΔE again be

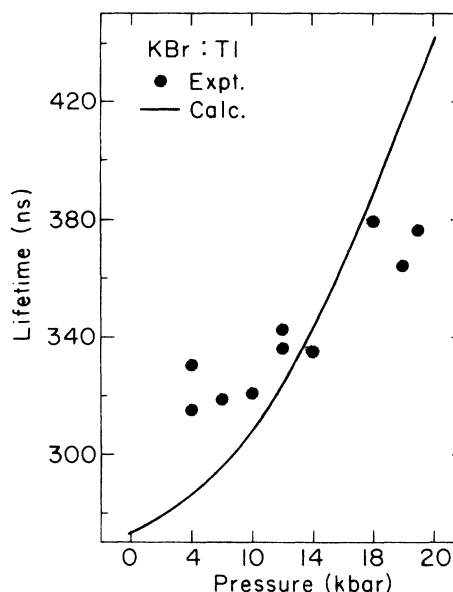


FIG. 11. Lifetime change with pressure for KBr:Tl at room temperature.

$E_T - E_X$, $\epsilon_X = E_X - E_{X_0}$, and $\epsilon_T = E_T - E_{T_0}$. Assuming no nonradiative paths, one arrives at an equation for the lifetime that is like Eq. (2)

$$\tau = \frac{1 + K + \frac{g_{X_0}}{g_X} \exp\left(\frac{\epsilon_X}{kT}\right) + \frac{g_{T_0}}{g_T} \exp\left(\frac{\epsilon_T}{kT}\right)}{k_X + Kk_T}, \quad (5)$$

where K is defined as before in Eq. (1). To reduce Eq. (5) to Trinkler's one-trap equation, one sets $g_{T_0} = 0$. Since traps take no part in steady-state emission, the expression for the peak-area ratio is still Eq. (2).

Proof that traps do not change steady-state data is provided by the steady-state plot of fcc KBr:Tl in Fig. 10. It is much the same as those seen previously, although the RT lifetime of KBr:Tl is trap dominated. From Fig. 10 we can again find $g_T \tau_X / g_X \tau_T$ and $\Delta E(p)$ (see Tables II and III). We find that $p_0 = 9$ kbar and $\%X(p_0) = 17\%$.

Lifetime data, however, are quite different from those of KH:In. Note that $\tau(p)$ rises in Fig. 11, instead of falling as before. The lifetime increases orders of magnitude as the temperature is lowered over our modest range, as in Fig. 12. Straight lines on such a plot of $\log_{10} \tau$ vs $1/kT$, imply that a single trap dominates the lifetime, which is given by Eq. (4). The slope of the line is $\epsilon \log_{10} e$ and the intercept is τ_{rad} . Below room temperature, the data in Fig. 12 do fall on lines. The problem is to show how Eq. (5) is approximated by the simpler Eq. (4) under certain conditions.

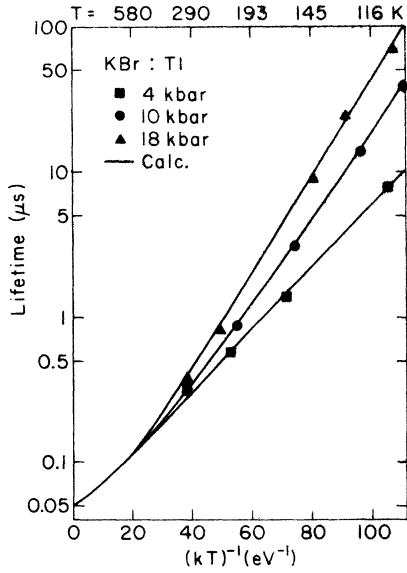


FIG. 12. Lifetime change with temperature for KBr:Tl at several pressures.

At atmospheric pressure, the trap depth in KBr:Tl measured from plots like Fig. 12 is 36 meV,¹⁷ or 40 meV.⁹ Then at temperatures lower than room temperature, the trap terms dominate Eq. (5); we see this domination throughout our temperature range in Fig. 12. At a pressure as high as 18 kbar, K is large so the $T0$ trap controls Eq. (5). Approximating, we find

$$\tau(18 \text{ kbar}) \approx \tau_T (g_{T0}/g_T) \exp(\epsilon_T^0/kT). \quad (6)$$

Fitting a line to the points in Fig. 12, one finds a trap depth $\epsilon_T = 77$ meV and an intercept $g_{T0}\tau_T/g_T = 0.02 \mu\text{sec}$.

Ten kbar is nearly p_0 , so Eq. (5) is simplified. Using the same value for $g_{T0}\tau_T/g_T$, but allowing the trap depth to change with pressure, one finds that $\epsilon_T = 69$ meV and $\epsilon_X \approx 49$ meV. At 4 kbar, ΔE is so large and positive ($\Delta E = 25$ meV) that the $X0$ trap controls Eq. (5). From the slope and intercept

of a line through the LT points of Fig. 12, one finds that $\epsilon_X = 43$ meV and $g_{X0}\tau_X/g_X = 0.05 \mu\text{sec}$. It appears that the trap depths do change with pressure, both increasing at a rate of about 1 meV/kbar.

Thus

$$\epsilon_X(\text{meV}) \approx 39 + p,$$

and

$$\epsilon_T(\text{meV}) \approx 59 + p, \quad (7)$$

where p is measured in kbar.

If we take a ratio of the intercepts found from Fig. 12, we find that

$$g_T\tau_X/g_X\tau_T = 2.5(g_{T0}/g_{X0}). \quad (8)$$

From the steady-state plot, we know that the quantity on the left in Eq. (8) is five, so $g_{T0}/g_{X0} = 2$. If the two traps are nondegenerate, or if a one-trap model is used, Eq. (8) leads to a factor-of-2 discrepancy. This is proof that a two-trap degenerate model must be used. Dang and Fukuda³ have written that the X level is generally doubly degenerate with an underlying nondegenerate trap. These assignments fit KBr:Tl if the T level is nondegenerate with an underlying doubly degenerate trap.

Once the degeneracies are assigned ($g_T, g_{X0} = 1$; $g_X, g_{T0} = 2$), intrinsic lifetimes can be found: $\tau_X = 100$ nsec and $\tau_T = 10$ nsec. With all parameters known (they are tabulated in Table V), curves are generated to fit $\tau(T)$ and $\tau(p)$ data, by using Eq. (5). The agreement in Fig. 12 is excellent. All the curves meet at $\tau = 50$ nsec, at infinite temperature. Note that the lifetime increases with pressure at every temperature (unlike the systems without traps). There are two reasons for this: (i) both traps become deeper at higher pressures; and (ii) on conversion from X to T emission, the deep $T0$ trap dominates the shallower $X0$ trap.

Figure 11 shows a calculation of RT $\tau(p)$ with the data. Agreement is good considering the expanded vertical scale. Using a degeneracy assignment of $g_X/g_T = 1$ in Fig. 11 gives slightly worse agreement, though it does not much affect Fig. 12. However,

TABLE V. Emission parameters of KBr:Tl.^a

$$\frac{g_T\tau_X}{g_X\tau_T} = 5, \quad \frac{g_{X0}\tau_X}{g_X} = 0.05 \mu\text{sec}, \quad \frac{g_{T0}\tau_T}{g_T} = 0.02 \mu\text{sec}, \quad \frac{g_{T0}}{g_{X0}} = 2, \quad \frac{g_X}{g_T} = 2, \quad \tau_X = 100 \text{ nsec}, \quad \tau_T = 10 \text{ nsec}.$$

Energy (meV)	Pressure (kbar)			
	0	4	10	18
ΔE	44.4	24.9	-4.37	-43.4
ϵ_X	39	43	49	57
ϵ_T	59	63	69	77

^aSymbols for the parameters are defined in Eq. (5).

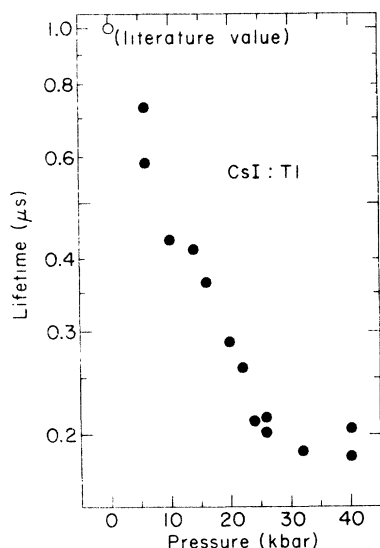


FIG. 13. Lifetime change with pressure for CsI:Tl at room temperature.

the trap degeneracy is certainly $g_{T0}/g_{X0} = 2$; any other assignment leads to a paradox.

Besides degeneracy assignments, some of the values in Table V are more certain than others. Trap depths ϵ_X (4 kbar) and ϵ_T (18 kbar) were measured, but their increase with pressure is given only by the fit to $\tau(T)$ data at 10 kbar. Thus, other trap depths are approximate. Similarly, ΔE was measured at 4 and 10 kbar, and other ΔE values are linear extrapolations. The main conclusion is that a trap must underlie each level X and T , and that the trap under the T level is doubly degenerate.

Extrapolations of this study to atmospheric pressure can be compared with two other experiments on KBr:Tl.^{9,17} Our intercept ($g_{X0}\tau_X/g_X$) of 50 nsec agrees with the values reported by the others [50 nsec (Ref. 9) and 67 nsec (Ref. 17)]. The extrapolation for ΔE of 44.4 meV is to be compared with 40 meV,¹⁷ that for ϵ_X of 39 meV is to be compared with 40 meV,⁹ and 36 meV.¹⁷ The three experiments are in accord.

The other Tl⁺-doped crystal which we studied is the CsI:Tl system. Drotning found three emitting peaks coexisting at 24 kbar. They are labeled (starting at lowest energy) 1, 2, and 3. At atmospheric pressure, only peak 1 is seen at room temperature. Peak 2 grows in with pressure until at 20 kbar it is larger than peak 1. To 30 kbar, peak 2 is largest, while 1 shrinks and peak 3 rises. Finally by 50 kbar and at higher pressure, only peak 3 is found. CsI has the sc structure at all pressures; there is no phase transition.

It is known from atmospheric pressure studies,¹⁹

that peak 2 grows in at lower temperatures down to 130°K. It turns out from our measurements that peak 2 rises as the temperature drops for every pressure from 0 to 40 kbar. Thus level 2 is at lowest energy throughout the pressure range studied. However, peak 2 is the largest peak only from 20 to 30 kbar at RT, because the intrinsic rate of emission from level 2 is much slower than for levels 1 and 3.

Since peaks 2 and 3 are probably analogs to peaks X and T , respectively,⁸ let us examine them first. Figure 10 shows a steady-state plot, where peak 2 takes the place of peak X . The situation is similar to the preceding plots because we are at pressures at which no emission from peak 1 is seen. One unusual feature is the large intercept (0.87). This means that $g_3\tau_2/g_2\tau_3 = 7.4$. For the sake of simplicity, assume that all levels are nondegenerate. Then τ_2 is 7.4 times slower than τ_3 . Levels 2 and 3 cross at $p_0 = 41$ kbar, where %2 = 12%.

The situation with lifetimes is more complicated. One might expect data similar to that of KBr:Tl, but from Fig. 13 it can be seen that the RT lifetime drops with pressure instead of rising. In Fig. 14, $\tau(T)$ curves do not tend toward a common intercept, as with KBr:Tl, though they are clearly trap dominated. Note that the dashed curves in Fig. 14 denote smoothed curves for the eye to follow, not calculation. It turned out that no calculations were possible for this system.

Equation (5) for a trap-dominated lifetime can be

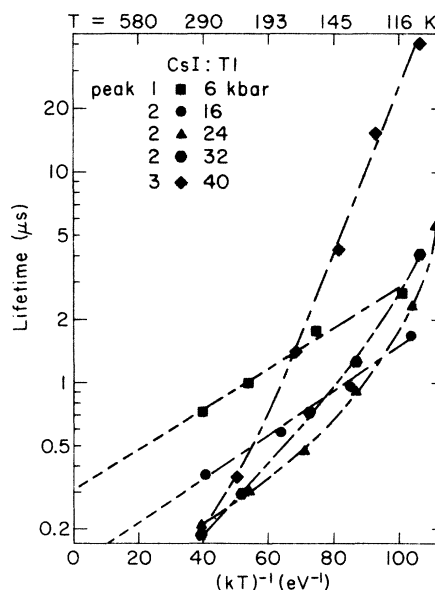


FIG. 14. Lifetime change with temperature for CsI:Tl at several pressures. Smoothed curves connect the data points.

TABLE VI. Parameters from linear fits to $\tau(T)$ data of CsI:Tl.

Pressure (kbar)	Slope/ \log_e (meV)	Intercept (nsec)
6	22.2	310.0
16	24.1	130
40	88.6	3.3

easily extended to the CsI:Tl case. For a general system of n emitting levels of energy E_i , each with an underlying metastable level E_{i0} at depth $\epsilon_i = E_i - E_{i0}$, all in "dynamic equilibrium," the measured lifetime is

$$\tau = \frac{\left[\sum_{i=1}^n g_i C_i + g_{i0} C_i \exp\left(\frac{\epsilon_i}{kT}\right) \right]}{\sum_{i=1}^n g_i C_i k_i}, \quad (9)$$

where $C_i = \exp(-E_i/kT)$. Depending on the C_i and ϵ_i , one trap or another may dominate at a particular pressure, in which case $\log_{10}\tau(T)$ is a straight line vs $1/kT$. That is the situation at 6, 16, and 40 kbar in Fig. 14. Table VI summarizes the slopes and intercepts found by fitting lines to the data.

At 24 and 32 kbar, one trap does not dominate the lifetime and data for $\tau(T)$ are curved. Looking at the slopes in Fig. 14, there appears to be a gentle slope (~ 20 meV) for low pressures and for 24 and 32 kbar at RT, giving way to a steep slope (~ 90 meV) for 40 kbar and for 24 and 32 kbar at Lt. The simplest theory would then have a shallow trap dominate the lifetime at low pressures and a deep trap at high pressures.

If $\tau(T)$ at 6 and 16 kbar is governed by the same trap (the slopes are the same), it is clear that an intrinsic rate must be increasing, since the $1/kT=0$ intercept in Fig. 14 drops. Even when three traps are considered, contradictions appear for the following reason: from the $1/kT=0$ intercept of 3.3 nsec at 40 kbar, τ_3 must be very fast. We know that τ_2 is 7.4 times slower than τ_3 at high pressure. From the $1/kT=0$ intercept of 310 nsec at 6 kbar, τ_1 must be very slow, and from steady-state measurements τ_2 is slower than τ_1 . Therefore τ_2 at high pressure must be ten times faster than at low pressure.

From Fig. 10 it appears that τ_2 and τ_3 are constant above 32 kbar. At low pressure, where peak 3 vanishes, a steady-state plot was attempted, but there was no common intercept. The intercept τ_2/τ_1 dropped with pressure, implying [like the $\tau(T)$ intercepts] that τ_2 drops with increasing pressure. A decrease with pressure of the intrinsic lifetime of τ_2 of level 2 would explain the falling $1/kT=0$ in-

tercepts in Fig. 14, if the intercepts are given by τ_2 and the trap underlies level 2. The same reasoning applies to the room-temperature lifetime (Fig. 13), which drops quickly at low pressure, where τ_2 is changing, and levels off at 30 kbar, where τ_2 must be constant by Fig. 10.

Thus a picture of the CsI:Tl system from 0 to 40 kbar would resemble the following: at low pressure, level 3 is very high and unpopulated; level 1 is just above level 2, which has an underlying shallow trap. At intermediate pressures, level 3 (which has an underlying deeper underlying trap) has dropped and level 1 has risen to an energy comparable with level 3. At high pressures, level 1 is very high and unpopulated, while level 3 is just above level 2. Since the trap under 3 is much deeper than the trap under 2, the former controls the lifetime at high pressures. In this latter situation, levels 2 and 3 behave like levels X and T in KBr:Tl, with τ_2 constant. However, as the pressure is lowered below 30 kbar, τ_2 rises by at least a factor of 10.

What causes the change in τ_2 ? A thermal quenching process is unlikely because according to the equations, this would not affect the low-pressure steady-state plot, which is affected. A non-radiative drain on level 2 would have an equal effect on levels 1 and 3, because of "dynamic equi-

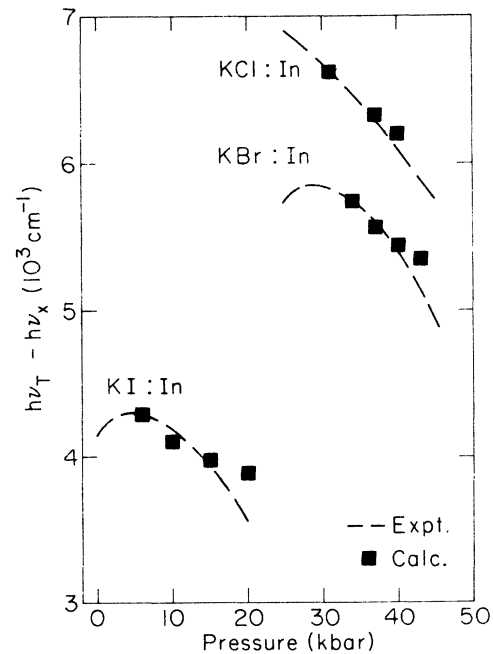


FIG. 15. Comparison of experimental and calculated values for the doublet energy separation vs pressure. Experimental curves were measured by Drotning and points are calculated from steady-state plots.

librium." That "equilibrium" applies is certain because barrier effects and fast components are seen only below 130°K in CsI:Tl and the RT lifetime is the same for all peaks. The drop in τ_2 must simply be due to a decrease in forbiddenness of emission from level 2.¹⁴

V. SUMMARY

In the potassium halides doped with In⁺, a simple two-level "equilibrium" model is found to explain the kinetics of the Jahn-Teller-split excited state. Several independent sets of data, including spectral and decay measurements versus pressure (0–60 kbar) and temperature (100–300°K), provide enough redundancy so that model parameters are well established. The *T* level, which at low pressure has a higher energy than the *X* level, falls until at high pressure it is more stable than the *X* level. The intrinsic radiative lifetime of the *X* state is longer than that of the *T* state. In sc KCl:In, the *X* level is doubly degenerate and the *T* level is nondegenerate, while in sc KBr:In, the *X* and *T* levels are equally degenerate.

Drotning's data for %*X* vs pressure showed that %*X* dropped from 100% to zero with increasing pressure. Calculations with the model using parameters from other data fit his points quite well (Fig. 2). In addition, Drotning published a graph similar to Fig. 15.⁸ The lines are smoothed curves through Drotning's data for the doublet separation. They are derived directly from experiment, and

thus are dashed to distinguish them from calculated curves which have been solid. The doublet separation is mainly due to a Stokes's shift, but the small decrease with pressure is due to the stabilization of the *T* level. Points in Fig. 15 are calculated from the measured JT splittings; values for ΔE from Table II are simply added to the Stokes's shift (assumed to be that at the lowest pressure). In other words, the calculated points are normalized to the experimental curve at the lowest pressure. Agreement between experiment and calculation is good, implying that nearly all information about the excited state wells is contained in the model.

In KBr:Tl and CsI:Tl, metastable levels from the Jahn-Teller-split ³A_{1u} manifold are found to dominate lifetime measurements. Parameters are extracted from KBr:Tl data for a four-level "equilibrium" model. The trap under the *T* level is deeper than and twice as degenerate as the trap under the *X* level. Behavior of the *X* and *T* levels is similar to that just described for In⁺. A six-level model could explain the CsI:Tl data but for the fact that the intrinsic radiative lifetime of one of the three emitting levels is found to be pressure dependent.

ACKNOWLEDGMENT

The authors would like to acknowledge the assistance of J. W. Hook III in taking the data of Fig. 7 and for useful discussions on the kinetics.

*Work supported in part by the U. S. ERDA under Contract No. EY-76-C-02-1198.

¹Atsuo Fukuda, Phys. Rev. B 1, 4161 (1970).

²A. Fukuda, A. Matsushima, and S. Masunaga, J. Lumin. 12,13, 139 (1976).

³L. S. Dang, R. Romestain, Y. M. d'Aubigné, and A. Fukuda, Phys. Rev. Lett. 38, 1539 (1977).

⁴A. Ranfagni, Phys. Rev. Lett. 28, 743 (1972).

⁵A. Ranfagni and G. Viliani, Phys. Rev. B 9, 4448 (1974).

⁶M. Bacci, A. Ranfagni, M. P. Fontana, and G. Viliani, Phys. Rev. B 11, 3052 (1975).

⁷M. Bacci, A. Ranfagni, M. Cetica, and G. Viliani, Phys. Rev. B 12, 5907 (1975).

⁸W. D. Drotning and H. G. Drickamer, Phys. Rev. B 13, 4576 (1976).

⁹Robert Illingworth, Phys. Rev. 136, A508 (1964).

¹⁰V. Gerhardt and W. Gebhardt, Phys. Status Solidi B 59, 187 (1973).

¹¹S. Benci, M. P. Fontana, and M. Manfredi, Phys. Status Solidi B 81, 603 (1977).

¹²W. D. Drotning and H. G. Drickamer, Phys. Rev. B 13, 4568 (1976).

¹³C. E. Tyner and H. G. Drickamer, J. Chem. Phys. 67, 4103 (1977).

¹⁴D. I. Klick, K. W. Bieg, and H. G. Drickamer, Phys. Rev. B 16, 4599 (1977).

¹⁵David Klick, Ph.D. thesis (University of Illinois, 1977).

¹⁶A. Nilisk and A. Laisaar, Phys. Status Solidi 33, 851 (1969).

¹⁷M. F. Trinkler *et al.*, Opt. Spectrosk. 19, 378 (1965) [Opt. Spectrosc. 19, 213 (1966)].

¹⁸M. F. Trinkler and I. K. Plyavin, Phys. Status Solidi 11, 277 (1965).

¹⁹S. Masunaga, I. Morita, and M. Ishiguro, J. Phys. Soc. Jpn. 21, 638 (1966).